High Voltage

Research Article

IET Journals
The Institution of Engineering and Technology

Estimation of de-trapped charge for diagnosis of transformer insulation using short-duration polarisation current employing detrended fluctuation analysis

eISSN 2397-7264
Received on 26th November 2019
Revised 11th April 2020
Accepted on 22nd April 2020
E-First on 8th June 2020
doi: 10.1049/hve.2019.0348
www.ietdl.org

Saurabh Dutta[1] ✉, *Deepak Mishra*[1], *Arijit Baral*[1], *Sivaji Chakravorti*[2]

[1]*Department of Electrical Engineering, Indian Institute of Technology (ISM), Dhanbad, India*

[2]*Department of Electrical Engineering, Jadavpur University, Kolkata, India*

✉ *E-mail: dutta.saurabh2@gmail.com*

Abstract: Researchers have shown that the value of charge carriers, de-trapped from the oil–paper interface of power transformer insulation, is useful in carrying out the diagnosis. However, the evaluation of the de-trapped charge requires the analysis of polarisation–depolarisation currents. Being an off-line time-consuming process, the measurement and analysis of polarisation and depolarisation current (PDC) data are not practically advantageous. The study presents a detrended fluctuation analysis-based technique to estimate the magnitude of normalised de-trapped charge using the polarisation current measured for a short duration. Using the proposed technique, the requirement of measuring the complete PDC data, for diagnosis purposes, can be eliminated. Further, the technique also eliminates the requirement of depolarisation current which in turn facilitates a reduction in equipment shutdown time. The applicability of the proposed technique is tested on the data obtained from several real-life power transformers.

1 Introduction

Ageing of oil–paper insulation is one of the main reasons behind high-voltage equipment failure [1, 2]. Some of the available techniques that are used for the condition assessment of power transformer insulation include dissolved gas analysis (DGA), degree of polymerisation (DP) analysis [3], time domain spectroscopy (TDS) and frequency domain spectroscopy (FDS) measurements [3]. The result of the DGA analysis, which involves the testing of transformer oil samples, depends significantly on the knowledge and expertise of the operator conducting the test [4]. Hence, the analysis of the same oil sample may lead to different results, depending on the operator. On the other hand, the DP value can provide accurate information about the condition of insulation [3]. However, the requirement of paper sampling from critical regions and the involvement of invasive testing make the DP value analysis unsuitable for real-life power transformers [3]. Techniques used for the condition assessment of in-service power transformers must be both reliable and non-invasive in nature [1]. Hence, the modification in existing non-invasive techniques for accurate estimation of the condition is always in demand. Popular non-invasive techniques involve the analysis of data obtained through TDS or FDS. It is reported in [1] that similar information regarding the insulation can be obtained from both TDS and FDS. However, the FDS measurement is a time-consuming technique especially in the low-frequency region [1–3]. In recent times, TDS-based techniques like the analysis of polarisation and depolarisation current (PDC) have become popular among utilities [1–3, 5–8]. It is reported in [3, 6] that a number of performance parameters can be estimated using the PDC data. However, the analysis of PDC data generally involves the formulation of insulation models. Non-unique insulation model parameters affect the reliability of diagnosis results [5]. Recent publications have shown that the effective analysis of the PDC data can be done without restoring to insulation model formulation. Such analysis usually involves the estimation and use of de-trapped charge [9, 10].

The real-life transformer insulation contains a large number of oil–paper layers. From a microscopic point of view, these oil–paper layers contain a large number of broken bonds. The positive charges being less mobile than negative charges get easily trapped at these broken bond sites present in the interfacial region [11–13]. This results in the creation of a potential barrier, where positive charges are trapped [12, 13]. The trapped charge carriers require a certain amount of energy to de-trap themselves from these trap sites [14, 15]. The energy required by the trapped charges to free themselves can be gained from thermal collisions, photon bombardment or electric field [16, 17]. Once the trapped charges become free by acquiring sufficient energy, they get absorbed at the electrode [9, 10]. This contributes to the overall conduction process and PDC measurement. Researchers in recent years have shown the capacity of de-trapped charge to act as a performance parameter [9, 10]. However, the estimation of the de-trapped charge requires a complete measurement of PDC [18, 19]. As per the existing literature, the de-trapping current does not influence the polarisation current due to the low applied field [19]. On the other hand, the depolarisation current profile does get affected by the charge de-trapping phenomenon that occurs at the interfacial region [19]. The magnitude of the de-trapped charge (obtained by integrating de-trapping current) can be used as an insulation sensitive parameter after removing the geometry effect [9, 10]. The complete measurement of PDC data requires measurement for about 20 000 s which is not at all beneficial for utilities [9, 10]. A method is reported in [20] which is capable of estimating the value of de-trapped charge using PDC data recorded for 1600 s (polarisation and depolarisation currents both measured for 800 s). Even tenure of 1600 s may prove to be demanding during the field measurement. This is because the magnitude of PDC data reduces to low values at a larger value of time and hence there is a chance that it might get affected by external noise [20] and temperature variation [21]. It is reported in [22] that estimation of complete polarisation current profile (up to 10 000 s) is possible using only 600 s of recorded data. However, this does not necessarily help in calculating the de-trapped charge as this requires the depolarisation current profile. Considering the above issues, a method is proposed which is capable of estimating the total de-trapped charge using only polarisation current recorded for 600 s. Unlike the technique described in [19], the proposed method neither requires depolarisation current nor does it require the estimation of the de-trapping current profile. This suggests that the proposed method significantly reduces the off-line data measurement time needed for

Table 1 List of transformers used for analysis

Transformer name	Transformer rating	Operational age	Meas. temp.
T1	420 kV/240 MVA	36	30.1
T2	400 kV/240 MVA	33	29.8
T3	420 kV/200 MVA	28	30.0
T4	420 kV/240 MVA	20	30.8
T5	400 kV/167 MVA	20	29.7
T6	400 kV/167 MVA	20	29.5
T7	420 kV/200 MVA	04	30.6
T8	420 kV/200 MVA	04	30.4
T9	420 kV/200 MVA	04	30.5
T10	765 kV/200 MVA	06	30.8
T11	765 kV/200 MVA	06	30.6
T12	420 kV/200 MVA	29	30.2
T13	220 kV/166 MVA	31	30.5
T14	220 kV/270 MVA	30	30.4
T15	420 kV/200 MVA	09	31.1
T16	765 kV/200 MVA	18	31.7
T17	420 kV/167 MVA	12	28.8

recording and analysis of dielectric response data for the estimation of the de-trapped charge.

It is a known fact that the dissipation factor (tanδ) gets directly influenced by the condition of the insulation [8, 23]. It is demonstrated in [23] that the value of tanδ shifts both vertically and horizontally with a change in measurement temperature w.r.t. the frequency axis [23]. It is a known fact that the profile of polarisation current and tanδ value get influenced by insulation conditions [1, 23]. Hence, in the present work, tanδ and a parameter (obtained after the application of detrended fluctuation analysis (DFA) [24] on the polarisation current profile) are utilised for the estimation of de-trapped charge. It has been observed that one of the parameters obtained after applying DFA to polarisation current maintains a well-defined relationship with normalised de-trapped charge and tanδ for any given transformer. This feature is utilised in developing the proposed methodology. The proposed methodology is developed using the data collected from a number of in-service power transformers mentioned in Table 1 (T1–T11). The developed technique is thereafter tested using the data collected from another set of real-life transformers (T12–T17 in Table 1) for validation purposes. It is worth mentioning here that the data obtained from transformers T12–T17 were not used at the initial development phase of the proposed methodology but are used solely for validation purposes.

PDC measurement being an off-line measurement technique [6], oil temperature that exists during the operation of a unit plays a minimal role in influencing the polarisation current profile. Prior to PDC measurement, the transformer is switched off and thereafter the unit is allowed sufficient cooling time [6] so that its internal temperature equalises with the ambient atmospheric temperature. As per the information provided by the utilities, each of the transformers mentioned in Table 1 was also allowed sufficient cooling time before PDC measurement was performed. Hence, the measurement temperature mentioned in Table 1 also happens to be the insulation temperature for a given unit.

2 Estimation of interfacial charge

A power transformer has a large number of oil–paper layers constituting a large amount of interfacial regions [25, 26]. The interfacial regions have a large amount of broken bonds forming trap sites for charge carriers. It is understood that during polarisation current measurement, only dielectric medium ionisation occurs [19]. During the polarisation phase, around 1000 V is applied across the insulation to avoid non-linearity in the system response [1]. For charge injection, a minimum of 10 kV/mm of field is required [12]. Hence, no charge injection occurs during polarisation current measurements. In recent studies, it has been demonstrated that normalised de-trapped charge Q_n has the capability to be used as a performance parameter [9, 10]. It is reported in [9] that Q_n maintains well-defined relationships with various performance parameters such as paper moisture content (%pm), %tanδ. Researchers in [10] have shown that the value of Q_n can be used to estimate the value of activation energy. Hence, it is understood that the estimation of Q_n is indeed important in order to estimate the condition of the transformer insulation. For utilities, it is of utmost importance that the condition of power equipment can be estimated and the related measurements are carried out within a very short time period. Measurements performed in a short duration of time are less prone to noise and are of less affected by ambient condition (such as temperature) variations. Hence, many researchers are engaged in finding ways to reduce the measurement time of various dielectric response spectroscopy for effective diagnosis of power transformer [22, 27]. It is worth mentioning here that the proposed algorithm not only eliminates the requirement of depolarisation current measurement, rather it also eliminates the estimation of the de-trapping current profile. It is reported that the trapped charge requires a certain amount of energy to get de-trap itself from the trap sites and contribute to depolarisation current measurement [19]. This energy is obtained from thermal oscillations [19]. After getting de-trapped from the trap sites, the charge carriers reach the electrodes, thus generating the de-trapping current. The de-trapping current contribution occurs during the depolarisation current measurement phase. As per available literature [19], the following conditions should be met for the estimation of de-trapping charge estimation:

(i) Charge is not injected from the electrodes during the polarisation current measurement.
(ii) It is assumed that the oil–paper insulation is a heterogeneous mixture and is composed of oil, paper and water types of dipoles. Also, the time taken for both polarisation and depolarisation is the same for a specific type of dipole group.

The de-trapping current contribution in the depolarisation current profile can be obtained by removing dipolar relaxation current using (1) [19]:

$$i_{dl} = i_{relax(dipole)} + i_{det} \tag{1}$$

In (1), i_{dl} represents the measured depolarisation current profile, $i_{relax(dipole)}$ is the current due to relaxation of dipoles on the application of charging voltage and i_{det} is the de-trapping current contribution in the depolarisation current profile. It is assumed [19] that the dipolar relaxation current $i_{relax(dipole)}$ contribution is similar in both PDCs. Equation (2) shows the relationship between i_{det} with polarisation current i_{pl} and i_{dl} considering the above assumption. DC conduction current i_{con} in (2) can be obtained using (3):

$$i_{pl} - i_{dl} = i_{con} - i_{det} \tag{2}$$

$$i_{con} = \left|i_{pl}(t_{ss})\right| + \left|i_{dl}(t_{ss})\right| \tag{3}$$

In (3), $\left|i_{pl}(t_{ss})\right|$ and $\left|i_{dl}(t_{ss})\right|$ represent the absolute steady-state values of i_{pl} and i_{dl}, respectively. As per the existing literature, the de-trapping current profile can be successfully approximated using three exponential decay functions as given by (4) [10]:

$$i_{det} = \sum_{i=1}^{3} P_i \times \exp(-t/\tau_i), \quad \tau_3 > \tau_2 > \tau_1 \tag{4}$$

In (4), P_1, P_2, P_3 represent the amplitude and τ_1, τ_2, τ_3 represent the time constant of different exponential functions used in modelling of i_{det} profile. These time constants (τ_1, τ_2, τ_3) signify different trap depths where the charges used to reside [10]. As per the method reported in [19], the total magnitude of the de-trapped charge is evaluated using the numerical integration of i_{det} profile. This method of estimating the value of de-trapped charge [utilising (1)–

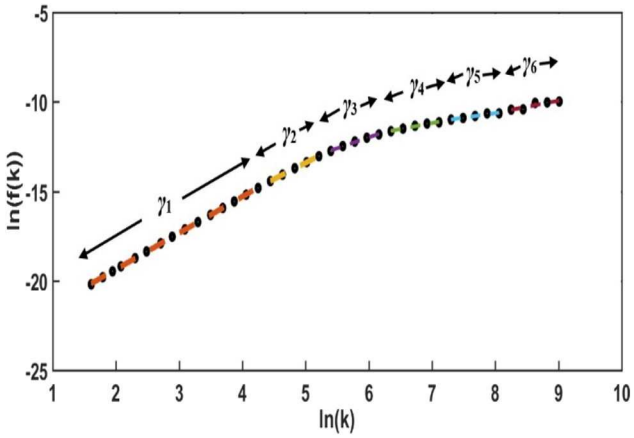

Fig. 1 *Plot of ln(f(k)) and ln(k) for γ calculation of T1*

(4)] is used during the formulation of the proposed relationship between de-trapped charge, tanδ, and DFA parameter. After the formulation of the proposed relationship, the method of estimating the de-trapped charge using (1)–(4) is not needed for the estimation of the de-trapped charge. In the proposed algorithm, first, the polarisation current is measured for 600 s. The methodology reported in [22] along with 600 s of measured polarisation current data is used for forecasting 10 000 s of polarisation current data. Thereafter, tanδ and result obtained after applying DFA on the forecasted polarisation current are used for further analysis.

The dissipation factor tanδ is widely used by the utilities for the assessment of the condition of the transformer insulation. Hence, tanδ along with a parameter obtained (using DFA) from the forecasted polarisation current profile has been used to estimate the value of Q_{n} in the proposed algorithm. Here, Q_{n} represents the value of normalised de-trapped charge. This de-trapped charge has been obtained after normalising the value of the de-trapped charge evaluated after integrating i_{det} [obtained in (4)]. It is worth mentioning here that the normalisation of the de-trapping charge has been done by multiplying $(1/(U_0C_0))$ with the de-trapping charge obtained using the method mentioned in Section 2 [18]. Here, U_0 is the charging voltage applied during polarisation current measurement and C_0 is the geometrical capacitance. The process of normalisation is done to reduce the geometry influence. The process of normalisation makes sure that the results obtained from different transformer units become comparable [18]. The value of tanδ used in the present work is measured using IDAX 300 and Tettex MIDAS.

To summarise, the following steps have been used to estimate the value of Q_{n} from tanδ and DFA parameter:

Step 1: Polarisation current for 600 s from several in-service transformers is recorded.
Step 2: Recorded 600 s polarisation current profiles are forecasted to obtain complete polarisation current profiles of 10 000 s.
Step 3: A suitably designed DFA tool is applied on 10,000 s of forecasted polarisation current profile.
Step 4: Finally, using tanδ (measured in Step 4) and DFA parameter (obtained in Step 3), the value of Q_{n} is evaluated.

In the next section, a brief discussion on the application of DFA (given in Step 3 of the proposed algorithm) to forecasted polarisation current profiles is provided.

3 Application of DFA

In the present work, DFA is applied to the forecasted polarisation current data to obtain a suitable parameter that follows some relationship with tanδ and Q_{n}. A suitably designed DFA has been applied to forecasted polarisation current data obtained from a number of real-life transformers. In DFA, initially the mean of the extracted detrended signal is subtracted from the original signal to eliminate the presence of the DC component from the signal. Thereafter, the signal is integrated as shown in (5):

$$y(l) = \sum_{j=1}^{l} x(j) - \overline{x(j)} \tag{5}$$

Further, the obtained signal is divided into K number of windows having equal number of data samples. Hence, the length of the window becomes $k = \mathrm{integer}(l/K)$, this helps in identifying the nature of fluctuation of the signal corresponding to a particular window, where l represents the number of data in the full signal under the test. Next, the local trend of the signal corresponding to each window is identified by applying the least-square method of order one. The trend signal corresponding to each window is represented by $y_{\mathrm{w}}(l)$. For identifying the deviation of the signal (corresponding to a particular window) from the whole integrated signal, an error is obtained corresponding to each window and is represented as $e(l)$ in (6):

$$e(l) = y(l) - y_{\mathrm{w}}(l) \tag{6}$$

In (6), $e(l)$ represents the detrended signal corresponding to a particular window. Whereas $y(l)$ and $y_{\mathrm{w}}(l)$ represent the entire integrated signal and trend signal corresponding to a specific window, respectively. In other words, the value of $e(l)$ provides information about the degree of deviation between the integrated signal $y(l)$ and the local trend signal given by $y_{\mathrm{w}}(l)$. The value of $e(l)$ corresponding to a small window size represents high-frequency fluctuations, whereas the value of $e(l)$ corresponding to a larger window size represents low-frequency fluctuations [24]. Depending on the nature of the test signal, the size of windows can be adjusted from small size to large size. In the present work, 10 000 s of forecasted polarisation current profile contains 30 000 samples and hence the size of the window is varied from 5 to 10 000. Finally, the root mean square error has been given by (7) corresponding to a particular window:

$$f(k) = \sqrt{\frac{1}{K.k}\sum_{w=1}^{K}\sum_{l=k(w-1)+1}^{w.k}(e(l))^2} \tag{7}$$

It is observed that with an increase in window size, the value of $f(k)$ increases. Available literature suggests that the relationship between window size K and function $f(k)$ can be modelled by the relationship of power law and can be expressed as $f(k) \simeq k^{\gamma}$, where γ represents the scaling parameter [24]. The value of γ gives the type of fluctuation in the original signal $x(j)$. The power law relation $f(k) \simeq k^{\gamma}$ can be plotted between ln(k) (as abscissa) and ln($f(k)$) (as ordinate), with γ as the slope of the curve. In the present work, six numbers of γ have been chosen from $\gamma 1$ to $\gamma 6$ with window sizes corresponding to $5 \le k \le 70$, $85 \le k \le 183$, $221 \le k \le 473$, $572 \le k \le 1224$, $1480 \le k \le 3166$, $3829 \le k \le 8188$, respectively. A plot of ln($f(k)$) and ln(k) showing the variation of $\gamma 1$–$\gamma 6$ is given in Fig. 1 for transformer T1. It is worth mentioning here that similar trends have been observed for other transformers.

4 Application of proposed methodology on in-service transformers

DFA parameters $\gamma 1$–$\gamma 5$ are observed to maintain a purely scatter relationship with Q_{n} and tanδ as shown in Figs. 2 and 3.

Figs. 2 and 3 further illustrate that DFA parameters $\gamma 1$–$\gamma 5$ do not follow any defined relationship with Q_{n} and tanδ. On the other hand, $\gamma 6$ is observed to maintain a good relation with tanδ (scaled by 20) and Q_{n}. This is illustrated in Fig. 4. To further investigate the relationship between data illustrated in Fig. 4, efforts are made to model the variation of DFA parameter ($\gamma 6$) with a tanδ and Q_{n} using standard equations (quadratic and three-parameter exponential equations). The obtained correlation coefficients are given in Table 2. The high value of the correlation coefficient

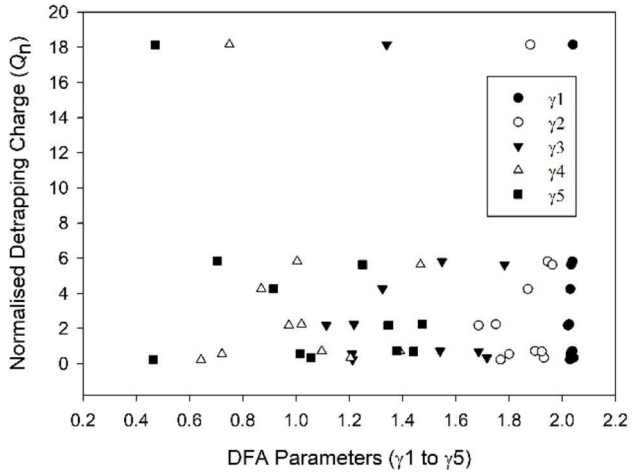

Fig. 2 *DFA parameters γ1–γ5 with Q_n for transformers T1–T11*

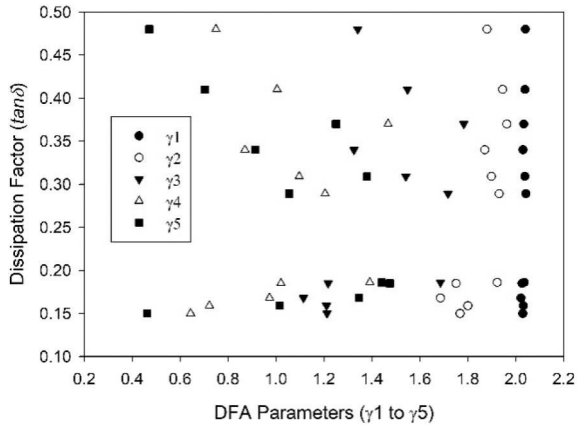

Fig. 3 *DFA parameters γ1–γ5 with tanδ for transformers T1–T11*

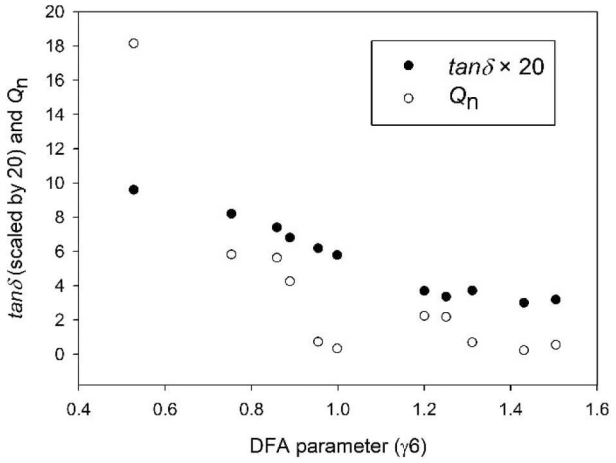

Fig. 4 *DFA parameter γ6 with tanδ (scaled by 20) and Q_n for transformers T1–T11*

Table 2 Correlation coefficient obtained by curve-fitting DFA parameter (γ6) with tanδ and Q_n using standard equations

Parameters	Corr. Coeff. obtained by curve-fitting using	
	Quadratic equation	Exponential equation
tanδ	0.9831	0.9819
Q_n	0.9499	0.9743

reinforces the fact that the DFA parameter (γ6) indeed maintains well-defined relationships with both tanδ and Q_n.

Table 3 Normalised de-trapping charge in tested transformers with tanδ and DFA parameter (γ6)

Transformer name	Norm. charge, Q_n	tanδ	DFA parameter (γ6)
T1	18.1400	0.4800	0.5277
T2	5.8200	0.4100	0.7538
T3	5.6300	0.3700	0.8588
T4	4.2600	0.3400	0.8888
T5	0.3375	0.2900	0.9984
T6	0.7227	0.3100	0.9542
T7	0.6979	0.1900	1.3107
T8	2.1816	0.1700	1.2502
T9	2.2392	0.1800	1.1996
T10	0.5561	0.1600	1.5043
T11	0.2255	0.1500	1.4303

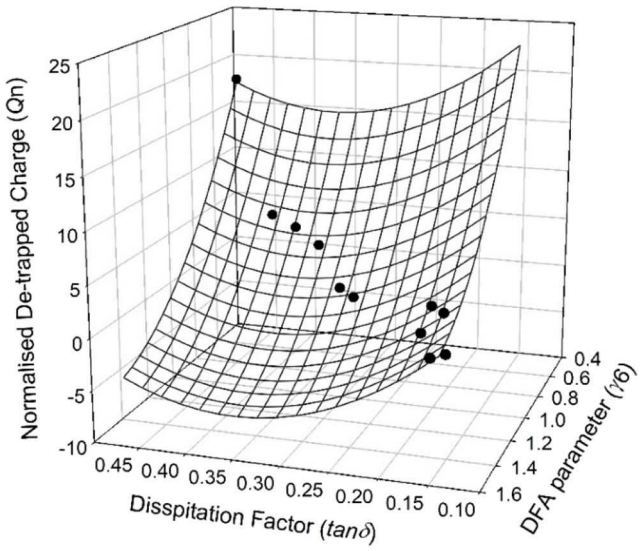

Fig. 5 *Three-dimensional scatter plot between tanδ, γ6 and Q_n*

Hence, parameter γ6 has been only used in subsequent analysis. The parameter γ6 along with the normalised de-trapping charge Q_n and tanδ (measured using IDAX 300 and Tettex MIDAS) for transformers T1–T11 have been given in Table 3.

It can be observed from the data given in Table 2 that the relationship that exists between tanδ and γ6 can be best modelled by a quadratic relationship. This relationship between tanδ and γ6 can be mathematically represented by (8):

$$\tan\delta = 0.8267 - 0.6966 \times \gamma 6 + 0.1567 \times (\gamma 6)^2 \quad (8)$$

To understand the relationship between γ6, Q_n and tanδ, a three-dimensional scatter plot is presented in Fig. 5 using the data given in Table 3. It is found that the scatter plot between Q_n, tanδ and γ6 shown in Fig. 5 maintains a well-defined relationship and can be modelled using (9):

$$Q_n = 64.55 - 127.04 \times \tan\delta - 59.30 \times \gamma 6 + 175.94 \times (\tan\delta)^2 + 17.93 \times (\gamma 6)^2 \quad (9)$$

It is worth mentioning here that the relationship is obtained for transformers having similar measurement temperature i.e. 30°C. Currently, the authors are engaged in collecting data measured at different temperatures, so that the relationship corresponding to other measurement temperatures (other than 30°C) can be constructed. To improve readability, the fitted surface is shown in Fig. 5. It is worth mentioning here that the least-square fitting has been applied in order to obtain the coefficients given in (9).

Using (9), the magnitude of Q_n can be calculated for known values of tanδ and γ6 corresponding to temperature 30°C.

Table 4 Values of Q_n obtained using reported [19] and proposed (9) technique along with tanδ and DFA parameter (γ6)

Transformer name	tanδ	DFA param. (γ6)	Norm. charge, Q_n (using [19])	Norm. charge, Q_n (using (9))	|%error|
T12	0.17	1.1268	3.7923	3.9840	5.05
T13	0.31	0.9493	1.8059	1.9399	7.42
T14	0.16	1.0878	5.1440	5.4379	5.71
T15	0.12	1.5370	2.8018	3.0519	8.93
T16	0.25	1.0693	0.9598	0.8780	8.52
T17	0.32	0.9185	2.7983	2.5729	8.05

Table 5 Values of ΔT for different transformers

Transformer name	Measurement Temp., Tp_1 (°C)	ΔT (°C)
T12	30.2	0.2
T13	30.5	0.5
T14	30.4	0.4
T15	31.1	1.1
T16	31.7	1.7
T17	28.8	1.2

$\Delta T = |Tp1 - 30|$.

Therefore, it can be understood that the magnitude of Q_n can be estimated using this relationship just by measuring 600 s of polarisation current data (instead of using complete polarisation current data). Hence, the proposed methodology eliminates the requirement of depolarisation current measurement. In addition to this, the proposed technique only uses 600 s of measured polarisation current data for the estimation of Q_n.

5 Validation of the proposed methodology

To validate the presented methodology, complete PDC data profiles (spanning 10 000 s) available for six numbers of in-service transformers (T12–T17) have been used. For these transformers, the values of tanδ were also obtained using IDAX 300 and Tettex MIDAS. It is worth mentioning here that the measurement temperature for these transformers was 30°C. The values of Q_n (given in the fourth column of Table 4) have been obtained using the technique explained in Section 2 [19] using complete measured profiles of PDC. This is done only for transformers T12–T17, especially for the purpose of validation. This value of the normalised de-trapped charge is assumed to be the actual value of Q_n for validation. The values of the DFA parameter γ6 were obtained using the forecasted polarisation current data (forecasted using 600 s of measured polarisation current data). The fifth column of Table 4 gives the values of Q_n calculated using tanδ, γ6 and (9). The values of Q_n along with tanδ and DFA parameter (γ6) are given in Table 4. It can be observed from the last column of Table 4 that |%error| between the values of Q_n (obtained using the proposed methodology) and that obtained using the technique reported in [19] is not substantial. The value of %error (given in the last column of Table 4) is calculated using the expression given in (10):

$$\%\text{error} = \frac{Q_n(\text{using [19]}) - Q_n(\text{using (9)})}{Q_n(\text{using [19]})} \quad (10)$$

Data presented in Table 4 shows that the proposed methodology is indeed capable of estimating the value of Q_n using a short duration polarisation current profile and even without measuring the depolarisation current profile. It can be observed from Table 4 that the proposed methodology is capable of providing an acceptable level of accuracy for transformers belonging to different age groups. However, the measurement temperature should be at 30°C. If the measurement temperature deviates from 30°C, suitable temperature compensation is required before the proposed methodology can be applied.

In order to improve the clarity, ΔT (deviation between measurement temperature Tp_1 and 30°C) corresponding to each transformer (mentioned in Table 4) is shown in Table 5.

It can be observed from Table 5 that, unlike T12–T14, the value of ΔT is more for T15–T17. Measurement temperature influences both polarisation current profile as well as tanδ value. This implies that inaccurate values of γ6 and tanδ have been used for obtaining Q_n for T15–T17 (shown in Table 4). It is understood from the above discussion that the accuracy of (9) will decrease with an increase in ΔT. Hence, |%error| values for these units are found to be slightly higher than those obtained for T12–T14. In case the temperature compensation is not done, the application of the proposed methodology can lead to a considerable error (illustrated in Table 4 for T15–T17). Furthermore, during the field measurement, it is practically difficult to ensure a particular measurement temperature owing to the different geographical location of transformers. Hence, a technique for temperature compensation is required for ensuring the reliability of the proposed method. Such a method is presented here that is capable of handling the issue related to variation in measurement temperature.

The method starts with polarisation current recorded for 600 s measured at temperature Tp_1 ($Tp_1 \neq 30$°C). Next, the technique reported in [22] is used to forecast the measured polarisation current data corresponding to Tp_1 to obtain the complete polarisation current profile (spanning 10 000 s). Thereafter, the forecasted polarisation current data at temperature Tp_1 is used to find the common debye model (CDM) parameters, using the method reported in [28]. It is reported in [23] that CDM parameters at any temperature can be estimated once the value of activation energy and CDM parameters (at a given measurement temperature) become known. Further, utilities generally assume the value of activation energy to be 1.15 eV [29]. Hence, in the present work, the value of activation energy is considered to be 1.15 eV.

By assuming the value of activation energy to be 1.15 eV and using the CDM (at Tp_1), the CDM parameters corresponding to temperature 30°C are calculated using the method reported in [23]. Thereafter, CDM corresponding to 30°C is used to obtain the complete polarisation current profile at 30°C using the method reported in [28]. Next, DFA is applied to the obtained polarisation current profile (corresponding to 30°C) and parameter γ6 is computed. Using γ6 (at 30°C) and (8), the value of tanδ (corresponding to 30°C) is obtained. Finally, using the relation given in (9) along with the values of tanδ and γ6 corresponding to 30°C, the value of Q_n is computed. For ease of understanding, the steps that are followed for obtaining Q_n at 30°C are given below:

Step 1: Polarisation current data is recorded for 600 s at a given measurement temperature (Tp_1).

Step 2: The measured polarisation current data is forecasted up to 10 000 s using the method given in [22].

Step 3: CDM is formulated using forecasted polarisation current data at Tp_1.

Step 4: Assuming the value of activation energy to be 1.15 eV and using the CDM (at Tp_1) obtained in Step 3, CDM at 30°C is obtained.

Step 5: Using CDM at 30°C, the polarisation current profile corresponding to 30°C is obtained.

Step 6: DFA parameter γ6 is computed by applying DFA to polarisation current data (obtained in Step 5).

Table 6 Values of Q_n after temperature compensation

Transformer name	ΔT (°C)	Norm. charge, Q_n (using (9))	Norm. charge, Q_n (using [19])	|%error|
T15	1.1	2.6760	2.8018	4.49
T16	1.7	0.9193	0.9598	4.22
T17	1.2	2.7121	2.7983	3.08

Step 7: Using (8) and $\gamma 6$, the value of tanδ (at 30°C) is computed.
Step 8: The value of Q_n corresponding to 30°C is calculated by substituting the values of $\gamma 6$, tanδ in (9).

The values of Q_n for T15–T17 obtained using the above-mentioned methodology are given in Table 6. Although the above-mentioned technique can be readily applied to all units shown in Table 4, T15–T17 are chosen for Table 6 as ΔT corresponding to these units are higher than those observed for T12–T14.

It can be observed from the last columns of Tables 4 and 6 that the values of |%error| have decreased after compensating the influence of measurement temperature. Hence, it can be opined that by using the temperature compensation technique mentioned above, the proposed methodology can be applied to data that are recorded under the influence of different measurement temperatures.

6 Conclusions

In the present work, a novel technique is presented to estimate the value of the de-trapped charge. From the presented technique, the following conclusions can be made:

- Normalised de-trapped charge forms a well-defined relationship with tanδ and DFA parameter at a given measurement temperature.
- The proposed methodology makes it possible to estimate the value of normalised de-trapped charge using short-duration polarisation current and tanδ.
- The proposed method is developed using short-duration measured PDC data (measured at 30°C) collected from real-life in-service units. Hence, it can be readily applied to other in-service units with PDC data measured at 30°C.
- A temperature compensation technique is also discussed using which it is possible to apply the proposed methodology to data that is recorded at temperatures other than 30°C.
- Using the proposed methodology, the requirement of measuring depolarisation current profile for the estimation of Q_n is eliminated. This reduces the off-line testing time for given equipment and hence reduces the overall shutdown time.
- The requirement of estimating the de-trapping current profile from depolarisation current involving (1)–(4) is eliminated. This implies that compared to available techniques, the presented method is less computationally extensive.
- The proposed method is capable of estimating the normalised de-trapped charge using only 600 s of measured polarisation current. This reduces the chance of polarisation current from getting effected by noise and temperature. Thus, ensuring the reliability and accuracy of the proposed method.

7 Acknowledgments

A. Baral and S. Chakravorti acknowledge the financial support provided by DST (SERB), GOI (grant no CRG/2018/001374).

8 References

[1] Zaengl, W.S.: 'Dielectric spectroscopy in time and frequency domain for HV power equipment, part I: theoretical considerations', *IEEE Electr. Insul. Mag.*, 2003, **19**, (5), pp. 5–19

[2] Zaengl, W.S.: 'Applications of dielectric spectroscopy in time and frequency domain for HV power equipment', *IEEE Electr. Insul. Mag.*, 2003, **19**, (6), pp. 9–22

[3] Saha, T.K.: 'Review of modern diagnostic techniques for assessing insulation condition in aged transformers', *IEEE Trans. Dielectr. Electr. Insul.*, 2003, **10**, (5), pp. 903–917

[4] Bakar, N.A., Abu-Siada, A., Islam, S.: 'A review of dissolved gas analysis measurement and interpretation techniques', *IEEE Electr. Insul. Mag.*, 2014, **30**, (3), pp. 39–49

[5] Banerjee, C.M., Saurabh Baral, A.: 'Influence of insulation model parameters on transfer function zero evaluated for diagnosis of oil-paper insulation'. 2017 3rd Int. Conf. on Condition Assessment Techniques in Electrical Systems (CATCON), Rupnagar, 2017, pp. 375–379

[6] Saha, T.K., Purkait, P.: 'Investigation of polarization and depolarization current measurements for the assessment of oil-paper insulation of aged transformers', *IEEE Trans. Dielectr. Electr. Insul.*, 2011, **11**, (1), pp. 144–153

[7] Gafvert, U., Adeen, L., Tapper, M.: 'Dielectric spectroscopy in time and frequency domain applied to diagnostics of power transformers'. Proc. 6th Int. Conf. Properties and Applications of Dielectric Materials (Cat. No.00CH36347), Xi'an, China, 2000, 2, pp. 825–830

[8] Linhjell, D., Lundgaard, L., Gafvert, U.: 'Dielectric response of mineral oil impregnated cellulose and the impact of aging', *IEEE Trans. Dielectr. Electr. Insul.*, 2007, **14**, (1), pp. 156–169

[9] Mishra, D., Haque, N., Baral, A., *et al.*: 'Effect of charge accumulated at oil–paper interface on parameters considered for power transformer insulation diagnosis', *IET Sci. Meas. Tech.*, 2018, **12**, (3), pp. 411–417

[10] Mishra, D., Dutta, S., Baral, A., *et al.*: 'Use of interfacial charge for diagnosis and activation energy prediction of oil-paper insulation used in power transformer', *IEEE Trans. Power Deliv.*, 2019, **34**, (4), pp. 1332–1340

[11] Wu, K., Zhu, Q., Wang, H., *et al.*: 'Space charge behavior in the sample with two layers of oil-immersed paper and oil', *IEEE Trans. Dielectr. Electr. Insul.*, 2014, **21**, (4), pp. 1857–1865

[12] Tang, C., Chen, G., Fu, M., *et al.*: 'Space charge behavior in multilayer oil-paper insulation under different DC voltages and temperatures', *IEEE Trans. Dielectr. Electr. Insul.*, 2010, **17**, (3), pp. 775–784

[13] Wang, S., Zhang, G., Mu, H., *et al.*: 'Effects of paper-aged state on space charge characteristics in oil-impregnated paper insulation', *IEEE Trans. Dielectr. Electr. Insul.*, 2012, **19**, (6), pp. 1871–1878

[14] Meunier, M., Quirke, N., Aslanides, A.: 'Molecular modeling of electron traps in polymer insulators: chemical defects and impurities', *J. Chem. Phys.*, 2001, **115**, (6), pp. 2876–2881

[15] Meunier, M., Quirke, N.: 'Molecular modeling of electron trapping in polymer insulators', *J. Chem. Phys.*, 2000, **113**, (1), pp. 369–376

[16] Chen, G., Xu, Z.: 'Charge trapping and detrapping in polymeric materials', *J. Appl. Phys.*, 2009, **106**, (12), p. 123707

[17] Zhou, T., Chen, G., Liao, R., *et al.*: 'Charge trapping and detrapping in polymeric materials: trapping parameters', *J. Appl. Phys.*, 2011, **110**, (4), p. 043724

[18] Dutta, S., Mishra, D., Haque, N., *et al.*: 'Influence of temperature on interfacial charge of power transformer insulation', *IET Sci. Meas. Tech.*, 2019, **13**, (7), pp. 1059–1067

[19] Mishra, D., Haque, N., Baral, A., *et al.*: 'Assessment of interfacial charge accumulation in oil-paper interface in transformer insulation from polarization-depolarization current measurements', *IEEE Trans. Dielectr. Electr. Insul.*, 2017, **24**, (3), pp. 1665–1673

[20] Mishra, D., Baral, A., Haque, N., *et al.*: 'Condition assessment of power transformer insulation using short duration time domain dielectric spectroscopy measurement data', *IEEE Trans. Instru. Meas.*, 2019, pp. 1–1, doi: 10.1109/TIM.2019.2947120 (accepted for publication). Early Access

[21] Saha, T.K., Purkait, P.: 'Investigations of temperature effects on the dielectric response measurements of transformer oil-paper insulation system', *IEEE Trans. Power Deliv.*, 2008, **23**, (1), pp. 252–260

[22] Mishra, D., Pradhan, A.K., Baral, A., *et al.*: 'Reduction of time domain insulation response measurement duration for fast and effective diagnosis of power transformer', *IEEE Trans. Dielectr. Electr. Insul.*, 2018, **25**, (5), pp. 1932–1940

[23] Dutta, S., Baral, A., Pradhan, A.K., *et al.*: 'Effect of measurement temperature on power transformer insulation diagnosis using frequency-domain spectroscopy', *IET Sci. Meas. Tech.*, 2017, **11**, (6), pp. 773–779

[24] Das, S., Pradhan, A.K., Kedia, A., *et al.*: 'Diagnosis of power quality events based on detrended fluctuation analysis', *IEEE Trans. Indus. Electro.*, 2018, **65**, (9), pp. 7322–7331

[25] Zhou, Y., Wang, Y., Li, G., *et al.*: 'Space charge phenomena in oil-paper insulation materials under high voltage direct current', *J. Electrost.*, 2009, **67**, (2), pp. 417–421

[26] Schmidt, W.: 'Electronic conduction processes in dielectric liquids', *IEEE Trans. Dielectr. Electr. Insul.*, 1984, **5**, (19), pp. 389–418

[27] Chatterjee, S., Pradhan, A.K., Dalai, S., *et al.*: 'Reducing frequency domain spectroscopy measurement time for condition monitoring of transformer oil-paper insulation using non-sinusoidal excitations', *IET Sci. Meas. Tech.*, 2017, **11**, (2), pp. 204–212

[28] Saha, T.K., Purkait, P., Müller, F.: 'Deriving an equivalent circuit of transformers insulation for understanding the dielectric response measurements', *IEEE Trans. Power Deliv.*, 2005, **20**, (1), pp. 149–157

[29] Emsley, A.M., Stevens, G.C.: 'Review of chemical indicators of degradation of cellulosic electrical paper insulation in oil-filled transformers', *IEE Proc. Sci., Meas. Tech.*, 1994, **141**, pp. 324–334